



**Providing Choice & Value**

Generic CT and MRI Contrast Agents



**FRESENIUS  
KABI**

**CONTACT REP**

**AJNR**

**Filtered Diffusion-Weighted MRI of the  
Human Cervical Spinal Cord: Feasibility and  
Application to Traumatic Spinal Cord Injury**

S.A. Murphy, R. Furger, S.N. Kurpad, V.E. Arpinar, A.  
Nencka, K. Koch and M.D. Budde

This information is current as  
of July 19, 2025.

*AJNR Am J Neuroradiol* published online 7 October 2021  
<http://www.ajnr.org/content/early/2021/10/07/ajnr.A7295>

# Filtered Diffusion-Weighted MRI of the Human Cervical Spinal Cord: Feasibility and Application to Traumatic Spinal Cord Injury

S.A. Murphy, R. Furger, S.N. Kurpad, V.E. Arpinar, A. Nencka, K. Koch, and M.D. Budde



## ABSTRACT

**BACKGROUND AND PURPOSE:** In traumatic spinal cord injury, DTI is sensitive to injury but is unable to differentiate multiple pathologies. Axonal damage is a central feature of the underlying cord injury, but prominent edema confounds its detection. The purpose of this study was to examine a filtered DWI technique in patients with acute spinal cord injury.

**MATERIALS AND METHODS:** The MR imaging protocol was first evaluated in a cohort of healthy subjects at 3T ( $n=3$ ). Subsequently, patients with acute cervical spinal cord injury ( $n=8$ ) underwent filtered DWI concurrent with their acute clinical MR imaging examination <24 hours postinjury at 1.5T. DTI was obtained with 25 directions at a b-value of 800 s/mm<sup>2</sup>. Filtered DWI used spinal cord–optimized diffusion-weighting along 26 directions with a “filter” b-value of 2000 s/mm<sup>2</sup> and a “probe” maximum b-value of 1000 s/mm<sup>2</sup>. Parallel diffusivity metrics obtained from DTI and filtered DWI were compared.

**RESULTS:** The high-strength diffusion-weighting perpendicular to the cord suppressed signals from tissues outside of the spinal cord, including muscle and CSF. The parallel ADC acquired from filtered DWI at the level of injury relative to the most cranial region showed a greater decrease (38.71%) compared with the decrease in axial diffusivity acquired by DTI (17.68%).

**CONCLUSIONS:** The results demonstrated that filtered DWI is feasible in the acute setting of spinal cord injury and reveals spinal cord diffusion characteristics not evident with conventional DTI.

**ABBREVIATIONS:** AD = axial diffusion; DDE = double diffusion encoding; fADC<sub>||</sub> = filtered parallel ADC; fDWI = filtered DWI; NODDI = neurite orientation dispersion and density imaging; PRESS = point-resolved spectroscopy sequence; SCI = spinal cord injury

Reliable biomarkers of spinal cord injury (SCI) severity could aid long-term functional prognosis and facilitate therapeutic decision-making. DWI has shown promise as a noninvasive tool to detect injury severity. DTI, the most widely used DWI model, has revealed important changes to the tissue microstructure that provide insight to function post-SCI in experimental models;<sup>1–6</sup> however, technical challenges and difficulties in interpreting the data are central reasons for the lack of DTI application within clinical settings and for investigations after human SCI.<sup>7–10</sup> To address these challenges, a recent

filtered DWI (fDWI) technique, originally developed on the basis of principles of double diffusion encoding (DDE), has shown promise in animal models<sup>3,11</sup> and simulations,<sup>12</sup> providing information about axonal injury after a spinal cord trauma. The purpose of this study was to examine the feasibility and efficacy of an fDWI scheme in the healthy human spinal cord with initial applications in the acutely injured cervical spinal cord.

DTI is uniquely sensitive to the microstructure of the spinal cord with an ability to reveal changes caused by injury that remain undetectable by other MR imaging schemes and contrasts. Axial diffusivity (AD), a directionally specific DTI metric quantifying diffusion parallel to the spinal cord, typically decreases after SCI and is specifically attributed to axonal damage.<sup>2</sup> In the acute SCI setting, decreased AD is likely caused by the formation of axonal beading that restricts water mobility,<sup>2,12–14</sup> though end-bulbs and other microscopic features of acutely injured axons may also contribute (Fig 1). Unfortunately, additional tissue responses to the injury, particularly edema and hemorrhage, confound AD measurements by DTI.<sup>15</sup> Edema is an evolving pathology in the early acute stage, and the logistics of patient transport and monitoring

Received February 8, 2021; accepted after revision July 7.

From the Department of Neurosurgery (S.A.M., R.F., S.N.K., M.D.B.), Center for Neurotrauma Research (R.F., S.N.K., M.D.B.), and Center for Imaging Research (V.E.A., A.N., K.K.), Medical College of Wisconsin, Milwaukee, Wisconsin.

This work was supported by the Craig H. Neilsen Foundation (546624) and a Merit Review Award (101RX002751) from the United States Department of Veterans Affairs Rehabilitation Research and Development Service.

Please address correspondence to Spencer A. Murphy, PhD, 8701 Watertown Plank Rd. Wauwatosa, WI 53226; e-mail: spamurphy@mcw.edu

Indicates open access to non-subscribers at www.ajnr.org

Indicates article with online supplemental data.

<http://dx.doi.org/10.3174/ajnr.A7295>

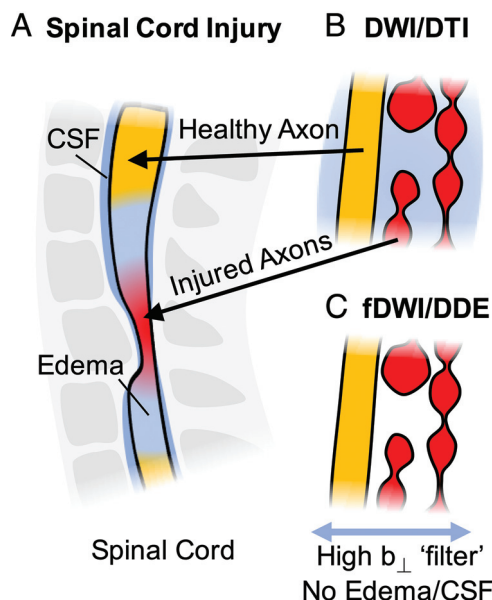


**FIG 1.** Schematic representation of the fDWI/DDE MR imaging technique for spinal cord injury. Traumatic injury to the spinal cord (A) results in microscopic damage to axons, illustrated here as beading and end-bulbs that reflect the underlying acute pathology (B). A prominent edema response (light blue) is typical surrounding the injury site. Traditional DWI/DTI derives measures reflecting the bulk sum of all features. With fDWI/DDE, a high-strength diffusion-weighting perpendicular to the spinal cord suppresses extracellular edema (and CSF) to estimate tissue-specific diffusivity metrics less confounded by edema.

after SCI complicate measures of edema.<sup>16,17</sup> Thus, a prominent limitation for the efficacy of DTI in the clinic is differentiating true axonal injury from the inflammatory response.

The goal of this study was to disambiguate healthy and injured axons using DWI. While DTI is confounded by extracellular edema,<sup>5</sup> through prior simulations and preclinical studies we have shown that the fDWI approach diminishes the effects of edema on the DWI metrics and is more sensitive to diffusion within axons (Fig 1). We compared AD measured by DTI with the filtered parallel ADC (fADC<sub>||</sub>) measured by fDWI within healthy and injured cords. Additionally, we used another DDE variant, a point-resolved spectroscopy sequence (DDE-PRESS) readout for single voxel, whole-cord measurements. The results demonstrated that both fDWI and DDE-PRESS are feasible MR imaging schemes with sensitivity to white matter diffusivity.

## MATERIALS AND METHODS

### Participants

All procedures were approved by the institutional review board at the Medical College of Wisconsin, and written consent was obtained from all participants. To first establish the protocol and demonstrate the feasibility on human systems, we tested the sequence on 3 healthy individuals with an intact spinal cord on a 3T scanner (mean age, 43.0 [SD, 16.4] years). Subsequently, the protocol was ported to a 1.5T clinical MR imaging system and evaluated in 8 patients with acute SCI (mean, 4.66 [SD, 3.23] hours from hospital admittance to scan time) (mean age, 51.9 ± [SD,

12.1] years). The Online Supplemental Data include participant characteristics.

### MR Imaging

For healthy subjects, cervical spine imaging was performed on a research-dedicated 3T Premier scanner with a 45-channel Head Neck Spine array (GE Healthcare). For subjects with acute SCI, imaging was performed on a clinical 1.5T Signa Optima MR450w GEM scanner with a 24-channel Head Neck Spine array (GE Healthcare). Participants were in the supine position with cushions/padding to limit head tilting and lordosis in the cervical (imaging) region. The participant was instructed to limit motion, such as swallowing, to breaks in the acquisition series.

To first characterize signal attenuation and illustrate the effects of diffusion filtering in the spinal cord, experiments in healthy subjects used diffusion-weighting perpendicular to the cord at b-values of 0, 200, 500, 1000, and 2000 s/mm<sup>2</sup>, using a pulsed gradient spin-echo acquisition with a diffusion separation ( $\Delta$ ) of 32.5 ms and duration ( $\delta$ ) of 25.4 ms. An EPI readout (TR = 2500 ms; TE = 64 ms) was used with an FOV of 200 mm<sup>2</sup> and 11 slices at a thickness of 5 mm and 0.2-mm gap.

For all participants, a DTI and fDWI protocol was used for an EPI readout. The DTI acquisition used 25 directions distributed along a sphere all at a b-value of 800 s/mm<sup>2</sup>. The diffusion-encoding for fDWI consisted of a diffusion-weighting “filter” gradient perpendicular to the spinal cord axis with a b-value of 2000 s/mm<sup>2</sup>. A separate diffusion-weighting “probe” gradient was applied parallel to the main axis of the spinal cord from 0 to 1000 s/mm<sup>2</sup>. A total of 26 directions was acquired that accounts for both a positive and negative combination of the filter and probe gradient directions. Scan times were similar for DTI and fDWI at 5 minutes 27 seconds and 5 minutes 35 seconds, respectively. For the healthy spinal cord, slices were centered at C4, while in the SCI group, slices were centered at the level of the lesion.

Because the diffusion filter pulse suppresses signals outside the spinal cord, the fDWI acquisition was additionally coupled with a single-voxel DDE-PRESS as a separate acquisition (TR = 2000 ms; TE = 145 ms). For individuals with SCI, this voxel (20 × 20 × 10 mm<sup>3</sup>) was placed at the epicenter of the lesion for 1 acquisition and above the lesion for a second acquisition, both maintaining alignment with the main axis of the spinal cord. The diffusion parameters for the DDE-PRESS sequence were identical to those in DWI-EPI to the extent possible. A b-value of 2000 s/mm<sup>2</sup> was used for the diffusion filter pair, and 9 different b-values from 0 to 2000 s/mm<sup>2</sup> in increments of 250 s/mm<sup>2</sup> were used for the diffusion probe (in addition to 1 non-diffusion-weighted spectrum). The full DDE-PRESS acquisition was repeated 4 times with a single average for each b-value and was acquired in 2 minutes 56 seconds. DDE-PRESS was performed on 6 of the 8 participants with SCI.

As part of the clinical MR imaging protocol, T2-weighted sagittal images were acquired and used for quantification of anatomic lesion features.

### Image Processing and Data Analysis

The Spinal Cord Toolbox (SCT; <https://spinalcordtoolbox.com/>) was used for the following postacquisition processing of the DWI-EPI data: 1) section-wise motion correction to correct for

translations in the axial plane; 2) DTI parameter maps of the whole FOV using linear least-squares fitting; 3) spinal cord segmentation; 4) spinal cord registration to the PAM50 template to automate ROIs for the CSF, gray matter, and white matter. Segmentation and registration were performed using the non-diffusion-weighted ( $b = 0 \text{ s/mm}^2$ ) image for DTI and the filtered, non-diffusion-weighted image ( $b = 2000 \text{ s/mm}^2$ ,  $b_{||} = 0 \text{ s/mm}^2$ ) for the fDWI acquisition. A pipeline was established to fully automate the tasks performed by the SCT, and the outputs were visually inspected to ensure its effectiveness and reliability. Mean cord values were obtained from the combined white and gray matter (ie, whole cord) because they could not be reliably discerned within the spinal cord injury setting, likely due to injury responses and the lower resolution on the 1.5T system. The noise and muscle ROIs were manually selected for healthy individuals and patients with SCI.

Maps of the diffusivity measured parallel to the cord in the presence of the perpendicular diffusion filter ( $fADC_{||}$ ) were estimated in Matlab (MathWorks) using a least-squares fit to the equation:

$$S_i = S_o \times \exp(-b \times D),$$

where  $S_o$  is the signal measured without diffusion-weighting and reflects the signal in the presence of the diffusion filter with no parallel diffusion weighting ( $b = 2000 \text{ s/mm}^2$ ,  $b_{||} = 0 \text{ s/mm}^2$ ),  $S_i$  reflects the measured signal at each of the  $b_{||}$ -values with  $b = q^2 \left( \Delta - \frac{\delta}{3} \right)$ . DTI and fDWI parameter maps were evaluated using an ROI analysis. Quantification of  $fADC_{||}$  and AD consisted of averages from each section and an average of all 11 slices for the specified ROI. Linear regression was used to relate  $fADC_{||}$  and AD across all slices for both the intact spinal cord group and the acute SCI group, with whole-cord values used for both groups for similar comparisons.

The average SNR of all slices within the ROIs was also measured and obtained from the non-diffusion-weighted images for DTI and fDWI by dividing images by the SD measured from a region of pure noise:

$$SNR = \frac{S_i}{SD(noise)}.$$

Analysis of DDE-PRESS data used custom Matlab scripts for derivation of diffusion parameters. The complex signals were Fourier-transformed, and the water peak within the single non-diffusion-weighted spectra ( $S_o$ ) was set as the frequency reference point for the subsequent integration of the other diffusion spectra. Integration of the absolute valued signal was performed between  $\pm 2 \text{ ppm}$  of the water peak to exclude the lipid contribution at approximately  $+3.5 \text{ ppm}$  from the water peak. The integrated and normalized signal ( $S_i/S_o$ ) was fit to a biexponential model:<sup>3</sup>

$$S_i = S_o \times f_R \times \exp(-b \times D_R) + S_o(1 - f_R) \times \exp(-b \times D_{fast}),$$

where  $D_R$  and  $D_{fast}$  capture the slow or restricted diffusion component ( $D_R$ ) and the fast or more freely diffusing component ( $D_{fast}$ ). The  $f_R$  reflects the fraction of the restricted signal. SNR was computed and defined as the mean signal divided by the SD from a region of pure noise.

The lesion length and hemorrhage extent were also measured from the cranial-to-caudal extents of the spinal cord hyperintensity and hypointensity, respectively, evaluated on sagittal T2-weighted images, consistent with the National Institutes of Health Common Data Elements.<sup>18</sup>

## Statistics

Statistical tests were performed using SPSS Statistics 27 (IBM). Data are reported as mean (SD). In the healthy subjects, a linear regression analysis was performed to compare  $fADC_{||}$  and AD across all slices from the same ROIs. A Wald-Wolfowitz runs test for randomness was used to determine whether linear regression was an appropriate fit to the data, with significance indicating the presence of a nonrandom distribution of residuals. For the subjects with acute injury, paired  $t$  tests were performed to compare each section with the most cranial section for each of the diffusivity metrics separately. The linear regression and runs test were also performed to directly relate  $fADC_{||}$  and AD. No direct comparisons between  $fADC_{||}$  and AD were performed because while they reflect similar features of parallel diffusivity, they are obtained from a different set of b-values and directions and are estimated differently using single-axis or tensor estimation.

## RESULTS

### Single-Axis Diffusion-Weighted Behavior in the Intact Spinal Cord

A pulsed gradient spin-echo applied perpendicular to the cord axis in the intact spinal cord exhibited a characteristic exponential decay within each of the tissue types captured by the ROIs (Online Supplemental Data). With increasing b-values, WM signal was less attenuated compared with that of the GM signal. There was nearly complete signal attenuation to the noise floor for the CSF and muscle at  $b = 2000 \text{ s/mm}^2$ . At the b-value  $2000 \text{ s/mm}^2$ , the mean SNR values from the WM (24.0 [SD, 3.4]) were greater compared with GM (14.0 [SD, 4.2]). The mean SNR for both CSF (6.77 [SD, 6.01]) and muscle (3.97 [SD, 4.10]) were indistinguishable from the noise floor (3.77 [SD, 2.11]). Collectively, these results demonstrate a diffusion gradient applied perpendicular to the cord ( $2000 \text{ s/mm}^2$ ) that resulted in a signal consisting primarily of spinal cord white matter without a contribution from non-neural tissues.

### Filter-Probe Diffusion-Encoding in the Intact Spinal Cord

In the intact cervical spinal cord, fDWI was compared with DTI (Fig 2). Mean  $fADC_{||}$  measured in the white matter ( $1.16 \text{ [SD, 0.38]} \mu\text{m}^2/\text{s}$ ) was lower compared with the mean AD ( $1.45 \text{ [SD, 0.40]} \mu\text{m}^2/\text{s}$ ) (Fig 2C), which equates to a reduction of 20.00%.

### Filter-Probe Diffusion-Encoding in the Injured Cervical Spinal Cord

fDWI, DTI, and DDE-PRESS were obtained in subjects with acute spinal cord injury. In a sample image of a single subject (Fig 3),  $fADC_{||}$  decreased at the injury site compared with AD. Averaged across all acquired slices, mean  $fADC_{||}$  values were lower ( $0.81 \text{ [SD, 0.42]} \mu\text{m}^2/\text{s}$ ) than mean AD values ( $1.36 \text{ [SD, 0.42]} \mu\text{m}^2/\text{s}$ ) (see examples for all participants in the Online Supplemental Data). A paired  $t$  test comparing each section with the most cranial section revealed a significant decrease at the injury epicenter



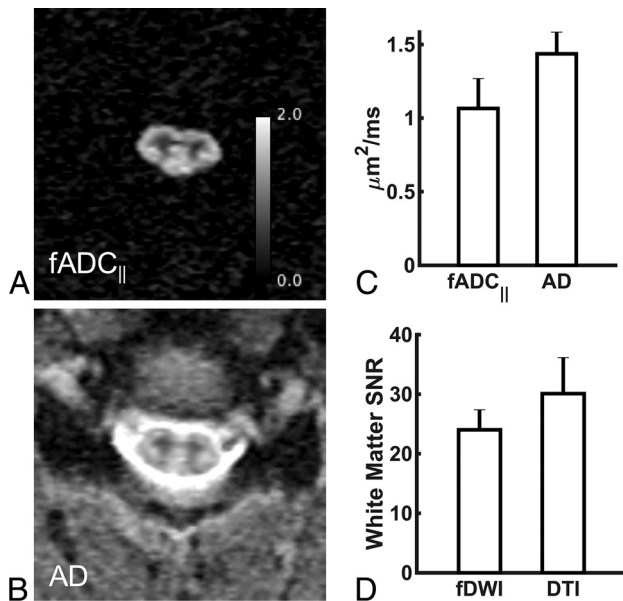


**FIG 2.**  $fADC_{||}$  and AD maps for the healthy spinal cord. Single-subject  $fADC_{||}$  (A) and AD maps (B) at C4 for a healthy individual on a 3T system. Comparison of the mean white matter  $fADC_{||}$  or AD values (C) and SNR (D).

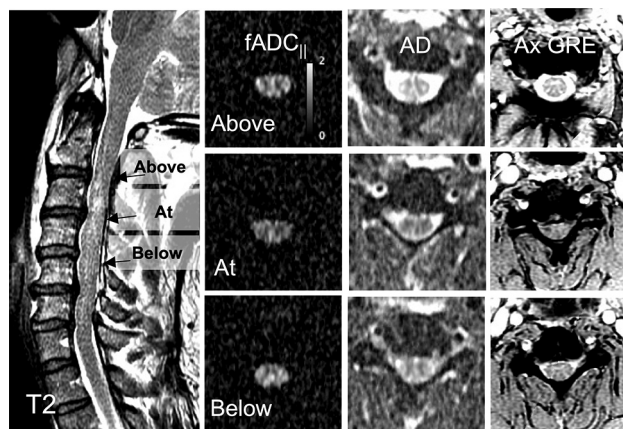


**FIG 3.**  $fADC_{||}$  and AD maps for an individual (subject 3) with an acute spinal cord injury. A T2-weighted image for an individual with an acute spinal cord injury on a 1.5T system. Single slices above, at, and below the injury site (as labeled in the T2 image) for  $fADC_{||}$  and AD maps. Ax GRE indicates axial gradient recalled-echo.

compared with above the injury for both  $fADC_{||}$ ,  $t(7) = 3.115$ ,  $P = .017$ , and AD,  $t(7) = 2.881$ ,  $P = .024$ . The most caudal section showed no significant differences compared with the most cranial section for  $fADC_{||}$ ,  $t(7) = 1.117$ ,  $P = .301$ , or AD,  $t(7) = -0.045$ ,  $P = .965$ . AD also decreased, though to a lesser extent, at the injury site compared with above and below the injury (Fig 4). When normalized to the first section above the injury,  $fADC_{||}$  values decreased an average of 38.71% at the injury epicenter, while AD decreased by 17.68% at the same section. However, AD also exhibited localized increases above and below the injury (Fig 5). Together, these results showed an overall decrease in diffusion measured parallel to the cord using 2 different DWI methods at the injury site, with a greater decrease in  $fADC_{||}$  compared with AD.

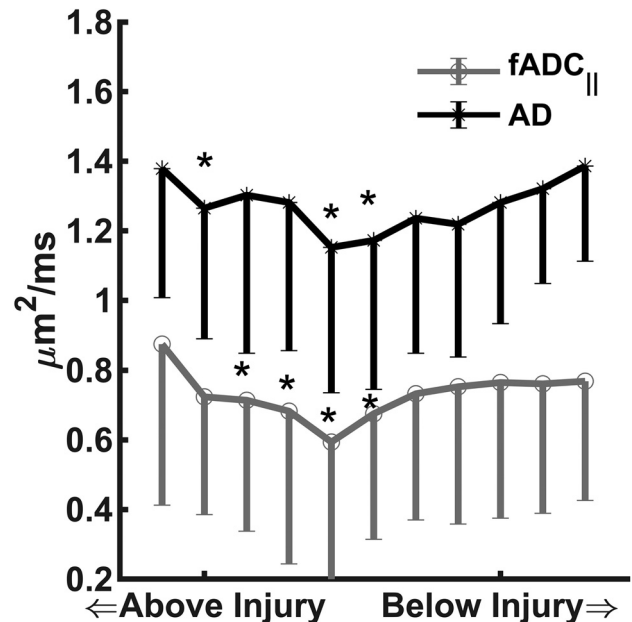


**FIG 4.**  $fADC_{||}$  and AD compared at each individual section for acute spinal cord injury ( $n = 8$ ). There is a large, unidirectional decrease in  $fADC_{||}$  at the injury site compared with a lesser, multidirectional decrease in AD values. The asterisk indicates significance compared with the first section ( $P < .05$ ).

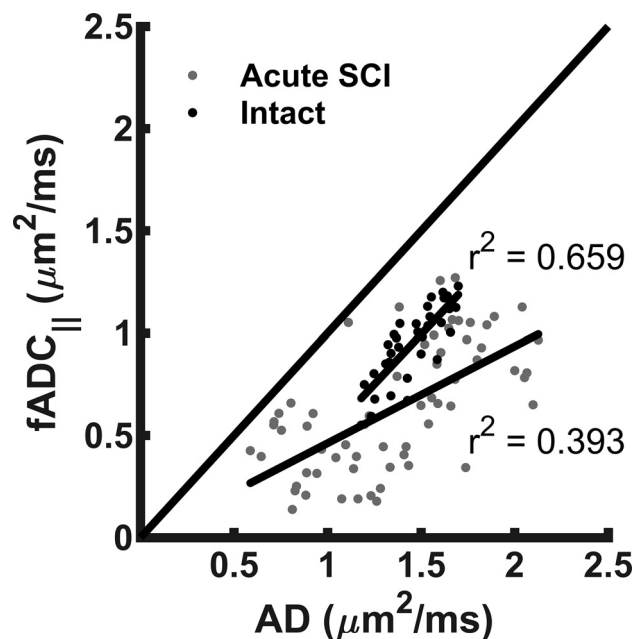


**FIG 5.** Correlations of  $fADC_{||}$  and AD at each individual section for the intact spinal cord and acute spinal cord injury. Correlations are significant for the intact spinal cord; however, a lower correlation and nonrandom residuals for the acute SCI setting indicate that  $fADC_{||}$  and AD do not have a simple linear relationship, suggesting that they provide differing information.

The relationship between  $fADC_{||}$  and AD was also evaluated to examine their differential effects. In the intact spinal cord,  $fADC_{||}$  and AD have a linear relationship with one another ( $r^2 = 0.659$ ,  $P < .001$ ) (Fig 5A), with a runs test confirming that the

residuals exhibit a random distribution ( $P = .344$ , Fig 5A). In acute injury,  $fADC_{||}$  and AD do not exhibit a similar relationship (Fig 5B) because the linear regression reveals a lower slope ( $r^2 = 0.393$ ,  $P < .001$ ), and the runs test indicates that the residuals are nonrandom ( $P < .001$ ). Together, these data showed that in the healthy, intact spinal cord,  $fADC_{||}$  and AD provide similar information, but after acute SCI, they exhibit differing information.

The same metric of  $fADC_{||}$  was also obtained from DDE-PRESS, though with differences in spatial positioning and coverage. In a patient with acute SCI (Online Supplemental Data), the EPI readout was complicated by artifacts and low image quality. However, the spectra exhibited a clear water peak and a lipid peak at both the injury site and above the injury site.  $fADC_{||}$  measured from DDE-PRESS demonstrated significantly lower mean values at the injury site ( $0.61$  [SD,  $33$ ]  $\mu m^2/ms$ ) compared with the more remote location above the injury ( $1.10$  [SD,  $0.34$ ]  $\mu m^2/ms$ ),  $t(5) = 2.89$ ,  $P = .034$ , showing trends similar to that of  $fADC_{||}$  obtained from EPI. These data together show that the estimated  $fADC_{||}$  from the DDE-PRESS for participants with low image quality was similar to that of fDWI.

## DISCUSSION

The results of this feasibility study demonstrated the efficacy and applicability of the filtered diffusion encoding scheme in the acute human spinal cord injury setting. The pathologic ambiguity of DTI hinders its utility to specifically evaluate axonal integrity in acute SCI.<sup>5,19</sup> The filtered diffusion approach exploits the spinal cord anatomy and known diffusion properties to suppress or filter predominantly extracellular signals as shown in prior animal and simulation studies.<sup>3,11,12</sup> In this study, we directly compared  $fADC_{||}$  measured by fDWI with AD measured by DTI in the same healthy subjects and a cohort of subjects with acute spinal cord traumatic injury. First, the results demonstrate that a b-value of  $2000\text{ s/mm}^2$  sufficiently suppressed signals outside the cord while retaining white matter signal (Fig 2). Second, decreases in  $fADC_{||}$  at the injury site of acute injury were more pronounced than those of AD. Similarly, while AD showed inconsistent fluctuations across the injured cord,  $fADC_{||}$  showed a unidirectional change compared with above and below the injury (Fig 5). Last, DDE-PRESS was able to capture similar measures of  $fADC_{||}$  indicative of axonal integrity for acute SCI (Online Supplemental Data), particularly useful in cases in which EPI quality was unusable.

In acute spinal cord injury, axonal integrity is believed to be the best indicator of functional outcome after a spinal cord injury,<sup>20</sup> and parallel or axial diffusivity is the diffusion metric most closely associated with the underlying cytotoxic edema consistent with swollen and beaded axons.<sup>2,12,21</sup> Indeed, in prior DTI studies of acute SCI, AD was the strongest correlate of long-term outcome.<sup>22</sup> The diffusion protocol in this study used multiple b-values along a single direction parallel to the spinal cord, enabling a more direct approach but with certain limitations. After traumatic SCI, axonal injury is also accompanied by a prominent edema response evident on T2-weighted images,<sup>23</sup> including both vasogenic or cytotoxic edema. Vasogenic edema is presumed to be extracellular, and as a consequence, it confounds DTI, resulting in counterintuitive increases in AD.<sup>2,12-14,24</sup> In the proposed fDWI approach,  $fADC_{||}$  has a minimal contribution from vasogenic edema and is more

specific to cytotoxic edema. These differential effects explain the greater sensitivity of  $fADC_{||}$  to the acutely injured cord (Fig 4).

Other approaches to resolving these diffusion properties have used multicompartment modeling of the diffusion signal. Notably, neurite orientation dispersion and density imaging (NODDI) is 1 example that estimates compartment volume fractions<sup>25</sup> but is based on the assumption of a single diffusion coefficient of  $1.7\text{ }\mu m^2/ms$  for the intra-axonal parallel diffusivity. This is likely to misattribute a prominent decrease in diffusivity to other estimated parameters. Furthermore, NODDI and other models require considerably more images for reliable estimates. Prior studies applying NODDI to the cervical spinal cord of patients with MS used approximately 18 minutes of imaging and nearly 100 images,<sup>26</sup> generally infeasible in a trauma setting. The primary advantage of fDWI in this context is that the filtering is achieved during data acquisition, improving feasibility. Moreover, fDWI has other favorable features including suppression of noncord tissue, most notably CSF and muscle. The suppression of CSF reduces artifacts attributable to motion such as CSF pulsation and reduces Gibbs ringing and partial volume effects in the spinal cord. Although fDWI inextricably has decreased SNR compared with similar DTI, it is countered by improvements in contrast and specificity.

The fDWI approach is also compatible with a straightforward single-voxel spectroscopic readout, and because noncord signals are suppressed, voxel dimensions can be larger than the cord axial cross-section. Previously,  $fADC_{||}$  derived from DDE-PRESS was shown to have a high degree of tolerance to magnetic field inhomogeneity artifacts that render EPI unusable.<sup>27</sup> In this study, similar results were evident in a subset of patients with poor EPI quality in which DDE-PRESS achieved decreased  $fADC_{||}$  values in the voxel at the injury site relative to one above the injury. As expected, DDE-PRESS sacrificed spatial information for greater SNR compared with EPI.

The primary limitation of this study is the small sample size. Further studies are needed in a larger cohort of patients and with long-term follow-up to appreciate the added value of fDWI in predicting neurologic outcome, because this is an important concern for both the patient and for improving stratification for clinical trials. This study was also limited in that healthy controls and patients with acute SCI were not scanned on the same magnet due to logistical limitations in equipment availability for the healthy population. Additionally, demonstrating the utility of these techniques within other clinical populations is needed. In particular, it may be suited to other conditions that impact the spinal cord such as multiple sclerosis and myelopathy, which have complex and evolving pathologies and in which diffusion metrics have been shown to be beneficial.<sup>28,29</sup>

## CONCLUSIONS

The results demonstrate that a diffusion acquisition tailored to the acutely injured spinal cord using filtered diffusion encoding improves sensitivity to white matter damage. The filtered diffusion metric  $fADC_{||}$  has a reduced dependence on vasogenic edema, and the results of this study show a greater decrease at the site of acute spinal cord injury compared with DTI metrics. Furthermore, a single-voxel method using the same diffusion filtering allowed estimates of  $fADC_{||}$  in cases in which more

conventional EPI had diminished quality. Future studies on a larger cohort of patients with acute and chronic SCI are needed to relate the improved sensitivity to functional outcomes. The fDWI scheme demonstrated in this study improved specificity to axonal damage, and it is believed that these advances will help in more accurately predicting long-term functional outcomes after spinal cord injury.

## ACKNOWLEDGMENTS

We would like to thank Victoria Slomski and all the MR imaging technologists at Froedtert Hospital and the Medical College of Wisconsin for acquiring the data in this study. We also thank Sarah Cornell for help recruiting patients to participate in the study.

Disclosures: Spencer A. Murphy—*RELATED: Grant:* The Craig H. Neilsen Foundation and Department of Veterans Affairs; *\* UNRELATED: Employment:* Medical College of Wisconsin. Robyn Furger—*RELATED: Grant:* The Craig H. Neilsen Foundation and Department of Veterans Affairs; *Comments:* grant to fund the research study. Shekar Kurpad—*UNRELATED: Grants/Grants Pending:* Bryon Riesch Paralysis Foundation; *\* Andrew Nencka—UNRELATED: Grants/Grants Pending:* GE Healthcare; *Comments:* My lab receives research funding from GE Healthcare for development, dissemination, and support of MR imaging pulse sequences for neurocognitive imaging studies. These pulse sequences were not used in the submitted work. *Stock/Stock Options:* VasoGnosis; *Comments:* I hold stock in a privately held company that focuses on image processing and communication in the field of neurovascular imaging of the head. No products or derivatives of work associated with that company were used in the submitted work. Kevin Koch—*UNRELATED: Grants/Grants Pending:* GE Healthcare; *Comments:* My lab receives research funding from GE Healthcare for development, dissemination, and support of MR technology development for orthopaedic and neurocognitive imaging studies. These technologies were not used in the submitted work. *Stock/Stock Options:* VasoGnosis; *Comments:* I hold stock in a privately held company that focuses on image processing and communication in the field of neurovascular imaging of the head. No products or derivatives of work associated with that company were used in the submitted work. \*Money paid to the institution.

## REFERENCES

- Zhao C, Rao JS, Pei XJ, et al. Longitudinal study on diffusion tensor imaging and diffusion tensor tractography following spinal cord contusion injury in rats. *Neuroradiology* 2016;58:607–14 [CrossRef Medline](#)
- Kim JH, Loy DN, Wang Q, et al. Diffusion tensor imaging at 3 hours after traumatic spinal cord injury predicts long-term locomotor recovery. *J Neurotrauma* 2010;27:587–98 [CrossRef Medline](#)
- Skinner NP, Kurpad SN, Schmit BD, et al. Rapid in vivo detection of rat spinal cord injury with double-diffusion-encoded magnetic resonance spectroscopy. *Magn Reson Med* 2017;77:1639–49 [CrossRef Medline](#)
- Patel SP, Smith TD, VanRooyen JL, et al. Serial diffusion tensor imaging in vivo predicts long-term functional recovery and histopathology in rats following different severities of spinal cord injury. *J Neurotrauma* 2016;33:917–28 [CrossRef Medline](#)
- Chiang CW, Wang Y, Sun P, et al. Quantifying white matter tract diffusion parameters in the presence of increased extra-fiber cellularity and vasogenic edema. *Neuroimage* 2014;101:310–19 [CrossRef Medline](#)
- Jirjis MB, Kurpad SN, Schmit BD. Ex vivo diffusion tensor imaging of spinal cord injury in rats of varying degrees of severity. *J Neurotrauma* 2013;30:1577–86 [CrossRef Medline](#)
- Cheran S, Shanmuganathan K, Zhuo J, et al. Correlation of MR diffusion tensor imaging parameters with ASIA motor scores in hemorrhagic and nonhemorrhagic acute spinal cord injury. *J Neurotrauma* 2011;28:1881–92 [CrossRef Medline](#)
- Cohen-Adad J, Buchbinder B, Oaklander AL. Cervical spinal cord injection of epidural corticosteroids: comprehensive longitudinal study including multiparametric magnetic resonance imaging. *Pain* 2012;153:2292–99 [CrossRef Medline](#)
- Vedantam A, Eckardt G, Wang MC, et al. Clinical correlates of high cervical fractional anisotropy in acute cervical spinal cord injury. *World Neurosurg* 2015;83:824–28 [CrossRef Medline](#)
- Shanmuganathan K, Zhuo J, Bodanapally UK, et al. Comparison of acute diffusion tensor imaging and conventional magnetic resonance parameters in predicting long-term outcome after blunt cervical spinal cord injury. *J Neurotrauma* 2020;37:458–65 [CrossRef Medline](#)
- Budde MD, Skinner NP, Muftuler LT, et al. Optimizing filter-probe diffusion weighting in the rat spinal cord for human translation. *Front Neurosci* 2017;11:706 [CrossRef Medline](#)
- Skinner NP, Kurpad SN, Schmit BD, et al. Detection of acute nervous system injury with advanced diffusion-weighted MRI: a simulation and sensitivity analysis. *NMR Biomed* 2015;28:1489–506 [CrossRef Medline](#)
- Budde MD, Frank JA. Neurite beading is sufficient to decrease the apparent diffusion coefficient after ischemic stroke. *Proc Natl Acad Sci U S A* 2010;107:14472–77 [CrossRef Medline](#)
- Steffensen AB, Sword J, Croom D, et al. Chloride cotransporters as a molecular mechanism underlying spreading depolarization-induced dendritic beading. *J Neurosci* 2015;35:12172–87 [CrossRef Medline](#)
- Sundberg LM, Herrera JJ, Narayana PA. In vivo longitudinal MRI and behavioral studies in experimental spinal cord injury. *J Neurotrauma* 2010;27:1753–67 [CrossRef Medline](#)
- Sliker CW, Mirvis SE, Shanmuganathan K. Assessing cervical spine stability in obtunded blunt trauma patients: review of medical literature. *Radiology* 2005;234:733–39 [CrossRef Medline](#)
- Leypold BG, Flanders AE, Schwartz ED, et al. The impact of methylprednisolone on lesion severity following spinal cord injury. *Spine (Phila Pa 1976)* 2007;32:373–78; discussion 379–81 [CrossRef Medline](#)
- Biering-Sørensen F, Alai S, Anderson K, et al. Common data elements for spinal cord injury clinical research: a National Institute for Neurological Disorders and Stroke project. *Spinal Cord* 2015;53:265–77 [CrossRef Medline](#)
- Surey S, Berry M, Logan A, et al. Differential cavitation, angiogenesis and wound-healing responses in injured mouse and rat spinal cords. *Neuroscience* 2014;275:62–80 [CrossRef Medline](#)
- Medana IM, Esiri MM. Axonal damage: a key predictor of outcome in human CNS diseases. *Brain* 2003;126:515–30 [CrossRef Medline](#)
- Fieremans E, Jensen JH, Helpert JA. White matter characterization with diffusional kurtosis imaging. *Neuroimage* 2011;58:177–88 [CrossRef Medline](#)
- Shanmuganathan K, Zhuo J, Chen HH, et al. Diffusion tensor imaging parameter obtained during acute blunt cervical spinal cord injury in predicting long-term outcome. *J Neurotrauma* 2017;34:2964–71 [CrossRef Medline](#)
- Leypold BG, Flanders AE, Burns AS. The early evolution of spinal cord lesions on MR imaging following traumatic spinal cord injury. *AJNR Am J Neuroradiol* 2008;29:1012–16 [CrossRef Medline](#)
- Williams PR, Marincu BN, Sorbara CD, et al. A recoverable state of axon injury persists for hours after spinal cord contusion in vivo. *Nat Commun* 2014;5:5683 [CrossRef Medline](#)
- Grussu F, Schneider T, Zhang H, et al. Neurite orientation dispersion and density imaging of the healthy cervical spinal cord in vivo. *Neuroimage* 2015;111:590–601 [CrossRef Medline](#)
- By S, Xu J, Box BA, et al. Application and evaluation of NODDI in the cervical spinal cord of multiple sclerosis patients. *Neuroimage Clin* 2017;15:333–42 [CrossRef Medline](#)
- Budde MD, Skinner NP. Diffusion MRI in acute nervous system injury. *J Magn Reson* 2018;292:137–48 [CrossRef Medline](#)
- Nukala M, Abraham J, Khandige G, et al. Efficacy of diffusion tensor imaging in identification of degenerative cervical spondylotic myelopathy. *Eur J Radiol Open* 2019;6:16–23 [CrossRef Medline](#)
- Farrell JA, Smith SA, Gordon-Lipkin EM, et al. High b-value q-space diffusion-weighted MRI of the human cervical spinal cord in vivo: feasibility and application to multiple sclerosis. *Magn Reson Med* 2008;59:1079–89 [CrossRef Medline](#)